

COMPUTATION OF PHONON DISPERSION IN NON-CRYSTALLINE
Mg-BASED ALLOYS

ADITYA M. VORA

*Parmeshwari 165, Vijaynagar Area, Hospital Road, Bhuj – Kutch, 370 001, Gujarat,
India*

E-mail address: voraam@yahoo.com

Received 6 March 2006; Revised manuscript received 19 February 2007

Accepted 15 December 2007 Online 8 February 2008

The computation of the phonon dispersion curves (PDC) and the related properties of three Mg-based metallic glasses, viz. $Mg_{70}Zn_{30}$, $Mg_{84}Ni_{16}$ and $Mg_{85.5}Cu_{14.5}$, are made using the well recognized model potential of Gajjar et al. The pseudo-alloy atom model is applied for the first time instead of the Vegard's law. The three theoretical approaches given by Hubbard-Beeby, Takeno-Goda and Bhatia-Singh are used in the present study to compute the PDC of the systems. Five local-field correction functions proposed by Hartree, Taylor, Ichimaru-Utsumi, Farid et al. and Sarkar et al. are employed for the first time to see the effects of exchange and correlation. The thermodynamic and elastic properties are computed from the elastic limits of the PDC and found to be in qualitative agreement with the available theoretical or experimental data. The present findings for the PDC of $Mg_{70}Zn_{30}$ alloy are found in fair agreement with available theoretical and experimental data.

PACS numbers: 63.50.+x, 65.60.+a

UDC 538.911, 539.31

Keywords: pair potential, metallic glasses, elasticity, phonons, thermodynamic properties, computer simulations

1. Introduction

In the last several decades, considerable theoretical development has taken place in the field of disordered condensed matter physics. Generally, in this field the disorder means periodic random structure. The few examples of such systems are the crystals with impurities, liquid metals, binary alloys, metallic glasses etc. The disordered materials are also known as non-crystalline materials. The metallic glasses play an important role in the field of materials science and engineering, which opens the door of research for both theoreticians and experimentalists. Such solids have electronic properties normally associated with the metals, but the atomic arrangements are not periodic. Most of the binary metallic glasses are made up of two metal

components, which are interesting systems for theoretical investigations. Based on the knowledge of interatomic interactions, we can understand the thermodynamic, mechanical and electronic transport properties of amorphous solids. Such investigations involve measurements of the collective density waves at larger momenta. For a few metallic glasses, it is possible to measure the dynamical structure factors up to very large wave vectors [1–4].

Keeping all this in mind, the theoretical computation of the phonon dynamics of three Mg-based metallic glasses, viz. $\text{Mg}_{70}\text{Zn}_{30}$, $\text{Mg}_{84}\text{Ni}_{16}$ and $\text{Mg}_{85.5}\text{Cu}_{14.5}$, are reported in the present article. Three main theoretical approaches, proposed by Hubbard-Beeby (HB) [5], Takeno-Goda (TG) [6] and Bhatia-Singh (BS) [7, 8] are used to compute the phonon frequencies of these metallic glasses.

The homovalent $\text{Mg}_{70}\text{Zn}_{30}$ glass is one of the most important candidates among simple metallic glasses. The dynamical properties of $\text{Mg}_{70}\text{Zn}_{30}$ glass have been reported theoretically by von Heimendl [9] using the equation of motion method, by Tomanek [10] using a model calculation, by Saxena et al. [11, 12] using the effective pair potential with TG approach, by Agarwal et al. [13] using BS and by Agarwal-Kachhava [13] using TG as well as BS approaches. Recently, Vora et al. [2, 3] and Thakore et al. [4] and have computed phonon dynamics of $\text{Mg}_{70}\text{Zn}_{30}$ glass with effective atom model with HB, TG and BS approaches. Experimentally, the PDC of $\text{Mg}_{70}\text{Zn}_{30}$ glass was studied by Suck et al. [15] for a few wave vector transfers near $q_P = 2.61 \text{ \AA}^{-1}$, at which the first peak is found in the static structure factor calculation. Hafner-Jaswal [16] and Hafner et al. [17] studied the atomic and electronic structure of $\text{Mg}_{70}\text{Zn}_{30}$ glass by using ab initio pseudopotential technique. Benmore et al. [18, 19] reported longitudinal excitations of the glass within the first pseudo-Brillouin zone using the neutron Brillouin zone technique at room temperature. The temperature dependence of the dispersion and damping coefficients of transverse excitations was studied by Bryk and Mryglod [20] using the method of generalized collective modes. The two-component $\text{Mg}_{84}\text{Ni}_{16}$ and $\text{Mg}_{85.5}\text{Cu}_{14.5}$ glasses are the candidates for the transition metal-simple metal group. The structural analysis of $\text{Mg}_{84}\text{Ni}_{16}$ glass has been studied by Nassif et al. [21], while the structural analysis of $\text{Mg}_{85.5}\text{Cu}_{14.5}$ glass has been reported by Nassif et al. [22]. A literature survey indicated that no one has reported the experimental or theoretical work related to phonon dynamics of $\text{Mg}_{84}\text{Ni}_{16}$ and $\text{Mg}_{85.5}\text{Cu}_{14.5}$ glasses.

In most of the above studies, the pseudopotential parameter is evaluated so that it generates a pair-correlation function or PDC, which is in good agreement with experimental data. Also, the Vegard's law [11, 12] was used to explain electron-ion interaction for binary metallic glasses. But it is well known that pseudo-alloy-atom (PAA) is a more meaningful approach to explain such kind of interactions in binary alloys and metallic glasses [1–4]. Hence, in the present article the PAA model is used to investigate the phonon dynamics of the binary glassy systems.

In the present computations, the three theoretical approaches, viz. HB, TG and BS, are adopted with the well recognized model potential of Gajjar et al. [1–3]. Five local-field correction functions due to Hartree (H) [23], Taylor (T) [24], Ichimaru-Utsumi (IU) [25], Farid et al. (F) [26] and Sarkar et al. (S) [27] are used for the first time in the present study of the screening influence on the aforesaid

properties. Besides, the thermodynamical properties, such as longitudinal sound velocity v_L , transverse sound velocity v_T , Debye temperature Θ_D , low temperature specific heat capacity C_V and some elastic properties, viz. the isothermal bulk modulus B_T , modulus of rigidity G , Poissons ratio σ and Youngs modulus Y are also calculated from the elastic limit of the PDC. Finally, the comparisons are made between the computed results and available theoretical as well as experimental data.

2. Computational methodology

The pair potential $V(r)$ is calculated from the relation given by [1–4],

$$V(r) = \left(\frac{Z^2 e^2}{r} \right) + \frac{\Omega_0}{\pi^2} \int F(q) \left[\frac{\sin(qr)}{qr} \right] q^2 dq, \quad (1)$$

where Z and Ω_0 are the valence and atomic volume of the glassy alloy, respectively.

The energy-wave number characteristics appearing in Eq. (1) are written as [1–4]

$$F(q) = \frac{-\Omega_0 q^2}{16\pi} |W_B(q)|^2 \frac{\varepsilon_H(q) - 1}{1 + [\varepsilon(q) - 1][1 - f(q)]}. \quad (2)$$

Here $W_B(q)$, $\varepsilon_H(q)$ and $F(q)$ are the bare ion model potential, the Hartree dielectric response function and the local field correction functions, respectively. In the present work, the local field correction functions due to H, T, IU, F and S are incorporated to see the impact of the exchange and correlation effects.

The well recognized model potential $W(q)$ of Gajjar et al. [1–4] in the real space, used in the present computation of phonon dynamics of binary metallic glasses, is of the form

$$\begin{aligned} W(r) &= \frac{-Ze^2}{r_C^3} \left[2 - \exp \left(1 - \frac{r}{r_C} \right) \right] r^2, & r \leq r_C, \\ &= \frac{-Ze^2}{r} & r \geq r_C. \end{aligned} \quad (3)$$

Here $U = qr_C$. This form has the feature of a Coulombic term outside the core and varying cancellation due to a repulsive and an attractive contribution to the potential within the core. Hence, it is assumed that the potential within the core should neither be zero nor constant, but it should vary as a function of r . Thus the model potential has the novel feature of representing varying cancellation of potential within the core over and above its continuity at $r = r_C$ and weak nature [1–4].

The theories for computing the phonon dynamics in amorphous solids, approaches proposed by Hubbard-Beeby (HB) [5], Takeno-Goda (TG) [6] and Bhatia-Singh (BS) [7, 8], have been employed in the present computation. The expressions for longitudinal phonon frequency and transverse phonon frequency as per HB, TG and BS approaches are given in Refs. [5–8].

According to HB, the expressions for the longitudinal phonon frequency ω_L and transverse phonon frequency are [5]

$$\omega_L^2(q) = \omega_E^2 \left[1 - \frac{\sin(q\sigma)}{q\sigma} - \frac{6 \cos(q\sigma)}{(q\sigma)^2} + \frac{6 \sin(q\sigma)}{(q\sigma)^3} \right], \quad (4)$$

and

$$\omega_T^2(q) = \omega_E^2 \left[1 - \frac{3 \cos(q\sigma)}{(q\sigma)^2} + \frac{3 \sin(q\sigma)}{(q\sigma)^3} \right], \quad (5)$$

where $\omega_E^2 = \left(\frac{4\pi\rho}{3M} \right) \int_0^\infty g(r)V''(r)r^2 dr$ is the maximum frequency.

Following TG [6], the longitudinal ω_L and transverse ω_T phonon frequencies are written as

$$\begin{aligned} \omega_L^2(q) = & \left(\frac{4\pi\rho}{3M} \right) \int_0^\infty g(r)dr \left[rV'(r) \left(1 - \frac{\sin(qr)}{qr} \right) \right. \\ & \left. + \{r^2V''(r) - rV'(r)\} \left(\frac{1}{3} - \frac{\sin(qr)}{qr} - \frac{2 \cos(qr)}{(qr)^2} + \frac{2 \sin(qr)}{(qr)^3} \right) \right] \end{aligned} \quad (6)$$

and

$$\begin{aligned} \omega_T^2(q) = & \left(\frac{4\pi\rho}{3M} \right) \int_0^\infty g(r)dr \left[rV'(r) \left(1 - \frac{\sin(qr)}{qr} \right) \right. \\ & \left. + \{r^2V''(r) - rV'(r)\} \left(\frac{1}{3} + \frac{2 \cos(qr)}{(qr)^2} + \frac{2 \sin(qr)}{(qr)^3} \right) \right] \end{aligned} \quad (7)$$

Recently, the BS [7] approach was modified by Shukla and Campnaha [8], they introduced screening effects. Then, with the above assumptions and modification, the dispersion equations for an amorphous material can be written as [7, 8]

$$\omega_L^2(q) = \frac{2N_C}{\rho q^2} (\beta I_0 + \delta I_2) + \frac{k_e k_{TF}^2 q^2 |G(qr_S)|^2}{q^2 + k_{TF}^2 \epsilon(q)} \quad (8)$$

and

$$\omega_T^2(q) = \frac{2N_C}{\rho q^2} \left(\beta I_0 + \frac{1}{2} \delta (I_0 - I_2) \right) \quad (9)$$

Here, M and ρ are the atomic mass and the number density of the glassy component, while $V'(r)$ and $V''(r)$ are the first and second derivatives of the effective pair potential, respectively. Other constants used in Eqs. (8) and (9) can be found in Refs. [7, 8].

In the long-wavelength limit of the frequency spectrum, both frequencies, viz. the longitudinal ω_L and the transverse ω_T phonon frequencies, are proportional to the wave vectors and obey the relationships

$$\omega_L \propto q \quad \text{and} \quad \omega_T \propto q, \quad \therefore \quad \omega_L = v_L q \quad \text{and} \quad \omega_T = v_T q. \quad (10)$$

where v_L and v_T are the longitudinal and transverse sound velocities of the glassy alloys, respectively. In the three approaches of this article, different expressions were used for the two velocities.

In the HB approach, the two velocities are given as [5]

$$v_L(HB) = \omega_E \sqrt{\frac{3\sigma^2}{10}} \quad (11)$$

and

$$v_T(HB) = \omega_E \sqrt{\frac{\sigma^2}{10}} \quad (12)$$

In the TG approach, the two velocities are given as [6]

$$v_L(TG) = \left[\left(\frac{4\pi\rho}{30M} \right) \int_0^\infty dr g(r)r^3 \{rV''(r) - 4V'(r)\} \right]^{1/2} \quad (13)$$

and

$$v_T(TG) = \left[\left(\frac{4\pi\rho}{30M} \right) \int_0^\infty dr g(r)r^3 \{3rV''(r) - 4V'(r)\} \right]^{1/2} \quad (14)$$

The expressions for v_L and v_T in the BS approach are [7, 8]

$$v_L(BS) = \left[\frac{N_C}{\rho} \left(\frac{1}{3} \beta + \frac{1}{5} \delta \right) + \frac{k_e}{3} \right]^{1/2}, \quad (15)$$

and

$$v_T(BS) = \left[\frac{N_C}{\rho} \left(\frac{1}{3} \beta + \frac{1}{15} \delta \right) \right]^{1/2}. \quad (16)$$

In the long-wavelength limit of the frequency spectrum, longitudinal, v_L , and transverse, v_T , sound velocities are computed. The isothermal bulk modulus B_T , the modulus of rigidity G , the Poissons ratio σ , the Youngs modulus Y and the Debye temperature θ_D were found using the expressions [1–4],

$$B_T = \rho \left(v_L^2 - \frac{4}{3} v_T^2 \right), \quad (17)$$

$$G = \rho v_T^2, \quad (18)$$

where ρ is the isotropic number density of the solid.

$$\sigma = 1 - \frac{2v_T^2/v_L^2}{2 - 2v_T^2/v_L^2}, \quad (19)$$

$$Y = 2G(\sigma + 1), \quad (20)$$

$$\theta_D = \frac{\hbar\omega_D}{k_B} = \frac{\hbar}{k_B} 2\pi \left[\frac{9\rho}{4\pi} \right]^{1/3} \left[\frac{1}{v_L^3} + \frac{2}{v_T^3} \right]^{-1/3} \quad (21)$$

where θ_D is the Debye frequency.

The low temperature specific heat C_V is obtained from Kovalenko-Krasny's expression [28],

$$C_V = \frac{\Omega_0 \hbar^2}{k_B T^2} \sum_{\lambda=L,T} \int \frac{d^3q}{(2\pi)^3} \frac{\omega_\lambda^2(q)}{\left[\exp\left(\frac{\hbar\omega_\lambda(q)}{k_B T}\right) - 1 \right] \left[1 - \exp\left(-\frac{\hbar\omega_\lambda(q)}{k_B T}\right) \right]}. \quad (22)$$

The basic feature of temperature dependence of C_V is determined by the behaviour of $\omega_\lambda(q)$.

3. Results and discussion

The input parameters and other constants used in the present computations are shown in Table 1. The thermodynamic and elastic properties of three Mg-based metallic glasses are given in Tables 2–4. The pair potentials, the phonon dispersion curves (PDC) and the heat capacities C_V of metallic glasses are displayed in Figs. 1–12.

TABLE 1. Input parameters and constants.

Glass	Z	N_C	M (amu)	Ω_0 (au)	ρ_M (g/cm ³)	r_C (au)
Mg ₇₀ Zn ₃₀	2.00	12.00	36.62	138.15	2.9699	1.0343
Mg ₈₄ Ni ₁₆	2.00	12.00	29.81	140.09	2.3837	1.0419
Mg _{85.5} Cu _{14.5}	1.85	12.00	29.99	144.95	2.3182	1.1008

The Mg₇₀Zn₃₀ glass is a special example of simple metallic glasses. The comparison of presently computed pair potentials with other such theoretical results [11, 13] is displayed in Fig. 1. From the figure, it is seen that the first zero of the pair potentials $V(r = r_0)$ due to the H-function occurs at $r_0 = 10.0$ au. But with the exchange and correlation, this zero shifts to $r_0 \leq 4.7$ au. The width of the pair potentials and the $V_{\min}(r)$ positions are also affected by the behaviour of the screening. It is also noticed that the well depth of presently computed pair potentials moved towards lower values of r as compared to those of Saxena et al. [11] and Agarwal-Kachhava [13]. The reported pair potentials [11, 13] show higher potential well depth, while present results generate lower potential well depth. Also, as we go from S- to H-screening, the depth positions of the pair potentials are shifted toward

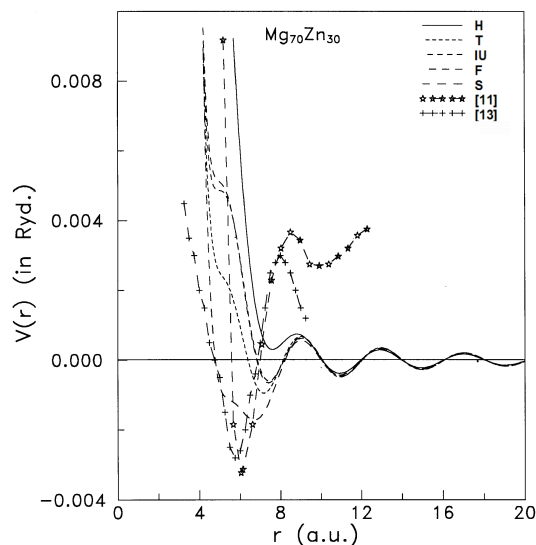


Fig. 1. Dependence on screening of pair potentials $V(r)$ of $Mg_{70}Zn_{30}$ glass. Legend: H – Hartree, T – Taylor, IU – Ichimaru-Utsumi, F – Farid et al., S – Sarkar et al.

higher r -values. The results of Saxena et al. [11] and Agarwal-Kachhava [13] show significant oscillations in their pair potentials and their potential energy remains almost positive in the large r -region. Thus, the Coulomb repulsive potential part dominates the oscillation due to the ion-electron-ion interactions in their studies. These types of oscillatory behaviour are also seen in the presently computed pair potentials.

The pair potentials of $Mg_{84}Ni_{16}$ glass are shown in Fig. 2. It is observed from the figure that the nature of the pair potentials is affected largely by the exchange and correlation effects. The position of the first minimum and first zero $V(r = r_0)$

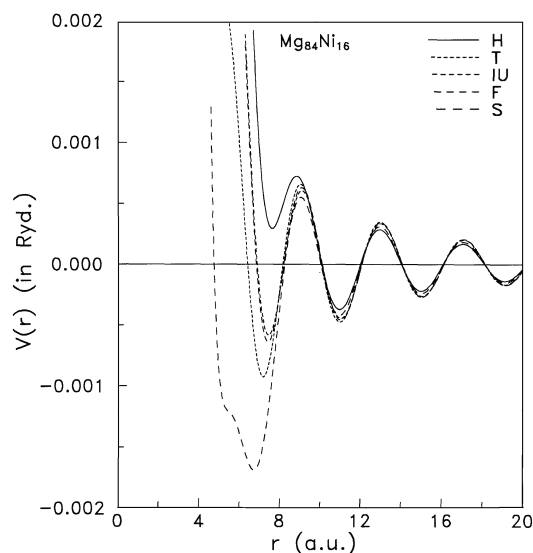


Fig. 2. Dependence on screening of pair potentials $V(r)$ of $Mg_{84}Ni_{16}$ glass. Legend: H – Hartree, T – Taylor, IU – Ichimaru-Utsumi, F – Farid et al., S – Sarkar et al.

of the pair potential due to H-function occurs at $r_0 = 10.1$ au, while the inclusion of the exchange and correlations suppresses this zero to $r_0 \leq 4.7$ au. The maximum depth of the pair potentials is obtained for the S-function, and behaviour of the pair potentials shows significant oscillations in the higher r -region. The computed pair potentials for $\text{Mg}_{85.5}\text{Cu}_{14.5}$ glass are shown in Fig. 3. It is seen from the figure that the behaviour of the pair potentials is very sensitive to the screening functions, particularly for the S-screening function. The pair potentials show soft-core nature. The first zero due to the H-function occurs at 10.5 au, while this zero due to other screenings occurs at $r_0 \leq 4.7$ au. The oscillatory behaviour is also seen in the presently computed pair potentials.

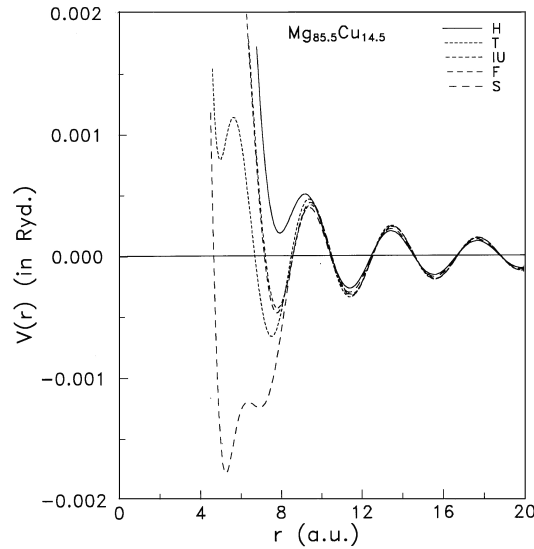


Fig. 3. Dependence on screening of pair potentials $V(r)$ of $\text{Mg}_{85.5}\text{Cu}_{14.5}$ glass. Legend: H – Hartree, T – Taylor, IU – Ichimaru-Utsumi, F – Farid et al., S – Sarkar et al.

One important feature noted from Figs. 1–3 regarding the pair potentials of the glassy alloys is that when we move from $\text{Mg}_{85.5}\text{Cu}_{14.5}$ to $\text{Mg}_{70}\text{Zn}_{30}$ glass, the valence, Z , of the glassy alloys increases and the depth positions shift towards higher r -values. That shows the strong dependence of the depth positions of pair potentials on the valence Z of the metallic glasses.

The influence of screening on the phonon frequencies of $\text{Mg}_{70}\text{Zn}_{30}$ glass in the HB approach are displayed in Fig. 4. The first minimum in the longitudinal branch is seen at $q \approx 1.6 \text{ \AA}^{-1}$ for the H-function and at $q \approx 2.6 \text{ \AA}^{-1}$ for the T-, IU- and F-functions, while at $q \approx 2.8 \text{ \AA}^{-1}$ for the S-function. At the first peak of the longitudinal phonon frequencies ω_L , the screening influence amounts to 68.88%, 57.58%, 61.12% and 72.76% for the T-, IU-, F- and S-functions, respectively, with respect to the static H-function. At the $q \approx 1. \text{ \AA}^{-1}$ point, such screening variations on the transverse phonon frequencies ω_T due to T-, IU-, F- and S-screening are 31.82%, 23.06%, 25.82% and 25.88%, respectively. The PDC computed from HB, TG and BS approaches with S-local field correction function are shown in Fig. 5. From the figure, it is seen that the first minimum in the longitudinal branches

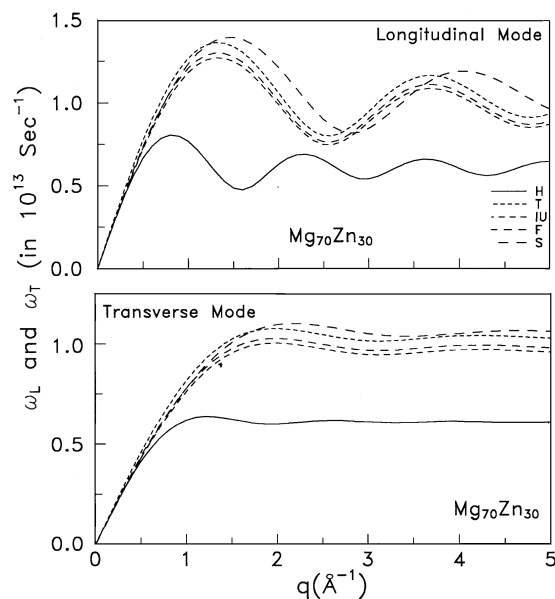


Fig. 4. Dependence on screening of phonon dispersion curves of $Mg_{70}Zn_{30}$ glass using HB approach. Legend: H – Hartree, T – Taylor, IU – Ichimaru-Utsumi, F – Farid et al. l., S – Sarkar et al.

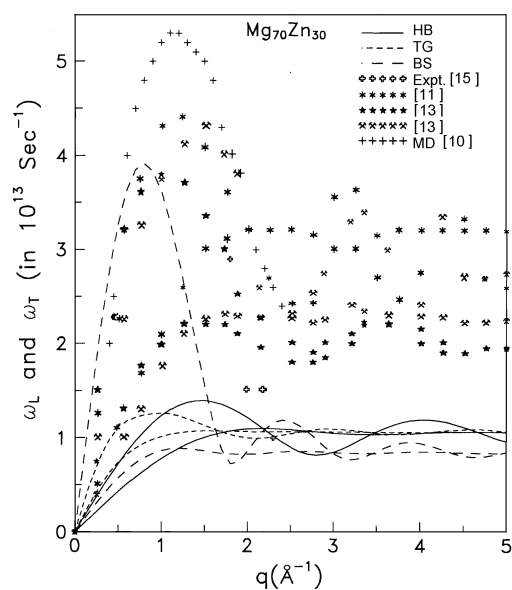


Fig. 5. Phonon dispersion curves of $Mg_{70}Zn_{30}$ glass using HB, TG and BS approaches with S -function. Legend: Expt. – experimental, MD – molecular dynamics.

occurs at $q \approx 1.8 \text{ \AA}^{-1}$ for the BS, $q \approx 2.9 \text{ \AA}^{-1}$ for the TG and $q \approx 2.8 \text{ \AA}^{-1}$ for the HB approach. The first crossing points of two-phonon branches ω_L and ω_T are observed at $q \approx 2.2 \text{ \AA}^{-1}$ in HB, at $q \approx 1.7 \text{ \AA}^{-1}$ in TG and at $q \approx 1.7 \text{ \AA}^{-1}$ in the BS approach. In comparison to the other reported theoretical [10, 11, 13] and experimental [15] data, the present results are suppressed but show qualitative

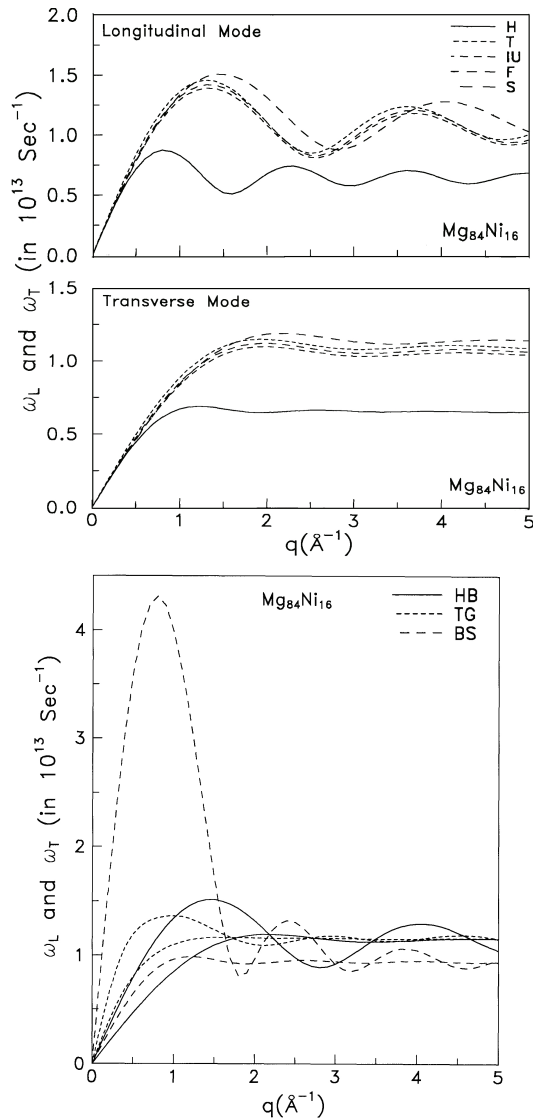


Fig. 6. Dependence on screening of phonon dispersion curves of $Mg_{84}Ni_{16}$ glass using HB approach. Legend: H – Hartree, T – Taylor, IU – Ichimaru-Utsumi, F – Farid et al., S – Sarkar et al.

Fig. 7. Phonon dispersion curves of $Mg_{84}Ni_{16}$ glass using HB, TG and BS approaches with S-function. Legend: HB – Hubbard-Beeby, TG – Takenogoda, BS – Bhatia-Singh.

agreement. The phonon frequencies for $Mg_{84}Ni_{16}$ glass obtained from various local-field correction functions with HB approach are displayed in Fig. 6. It is seen from the figure that the first minimum in the longitudinal branches occurs at $q \approx 1.6 \text{ \AA}^{-1}$ for the H-function, at $q \approx 2.6 \text{ \AA}^{-1}$ for the T-, IU-, F-functions and at $q \approx 2.8 \text{ \AA}^{-1}$ for the S-function. At the first maximum, the screening influence on ω_L is 62%–71% with respect to the static H-dielectric function. That influence on ω_T at $q \approx 1.0 \text{ \AA}^{-1}$ is 24%–32%. The PDC due to HB, TG and BS approaches with S-local field correction function are shown in Fig. 7. It is noticed that the oscillations are more prominent in the longitudinal phonon modes as compared to the transverse

modes. The phonon frequencies due to the BS approach are more enhanced than in the HB and TG approaches. The first minimum in the longitudinal branches occurs at $q \approx 1.8 \text{ \AA}^{-1}$ for BS, $q \approx 2.1 \text{ \AA}^{-1}$ for TG and $q \approx 2.8 \text{ \AA}^{-1}$ for the HB approach. The first crossover points of ω_L and ω_T in the three approaches are observed at $q \approx 2.2 \text{ \AA}^{-1}$, $q \approx 1.7 \text{ \AA}^{-1}$ and $q \approx 1.7 \text{ \AA}^{-1}$, respectively.

Figure 8 shows, the graphical representation of the PDC of $\text{Mg}_{85.5}\text{Cu}_{14.5}$ glass using HB approach with five screening functions, while Fig. 9 represents the com-

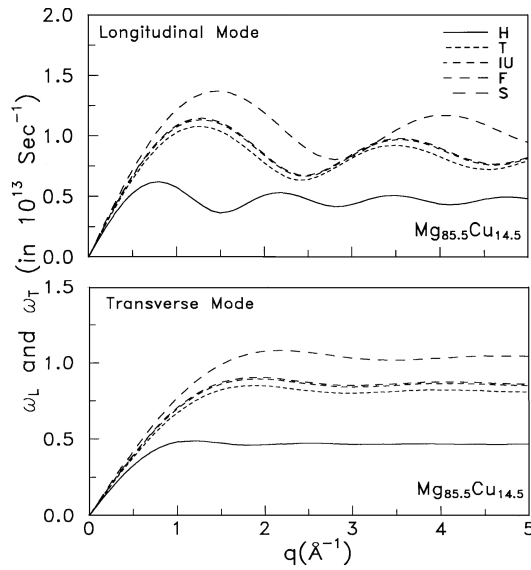


Fig. 8. Dependence on screening of phonon dispersion curves of $\text{Mg}_{85.5}\text{Cu}_{14.5}$ glass using HB approach. Legend: H – Hartree, T – Taylor, IU – Ichimaru-Utsumi, F – Farid et al., S – Sarkar et al.

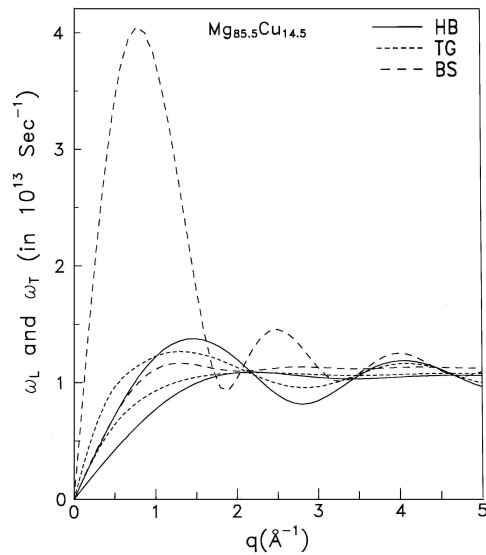


Fig. 9. Phonon dispersion curves of $\text{Mg}_{85.5}\text{Cu}_{14.5}$ glass using HB, TG and BS approaches with S-function. Legend: HB – Hubbard-Beeby, TG – Takeno-Goda, BS – Bhatia-Singh.

parative study of PDC generated through the three approaches, HB, TG and BS, with the S-local field correction function. It is seen from Fig. 8 that the inclusion of screening functions enhanced phonon frequencies in comparison with the static H-dielectric function. The first minimum in the longitudinal branches is found at $q \approx 1.6 \text{ \AA}^{-1}$ for H, at $q \approx 2.4 \text{ \AA}^{-1}$ for T, at $q \approx 2.6 \text{ \AA}^{-1}$ for IU, F and at $q \approx 2.8 \text{ \AA}^{-1}$ for the S-screening function. The influence of various local field correction functions at the first peak of longitudinal modes are 73.82% for T, 82.86% for IU, 84.96% for F and 121.27% for the S-function with respect to the H-function. Such screening influence on ω_T at the $q \approx 1.7 \text{ \AA}^{-1}$ position amounts to 39.43%, 44.84%, 46.52% and 59.53% for T, IU, F and S-screening functions, respectively. It is apparent from Fig. 9 that the longitudinal phonon frequencies show stronger oscillatory behaviour in the large q -region, what means the existence of collective excitations of large momentum transfer, while transverse modes show hardly any oscillations in the higher q -region, which suggests that transverse phonon behaviour is monotonic. Moreover, the present results for longitudinal phonon frequencies ω_L due to the BS approach are very much higher than those of the HB and BS approaches. The first minimum in the longitudinal branch occurs at $q \approx 1.8 \text{ \AA}^{-1}$, $q \approx 2.8 \text{ \AA}^{-1}$ and $q \approx 2.8 \text{ \AA}^{-1}$ for the BS, TG and HB approaches, respectively. The first crossover points of two-phonon branches in the HB, TG and BS approaches are observed at $q \approx 2.2 \text{ \AA}^{-1}$, $q \approx 2.2 \text{ \AA}^{-1}$ and $q \approx 1.4 \text{ \AA}^{-1}$, respectively.

Also, one important feature noted from Figs. 4–9 of the PDC of the glassy alloys, is that when we move from $\text{Mg}_{85.5}\text{Cu}_{14.5}$ to $\text{Mg}_{70}\text{Zn}_{30}$ glass, valence Z of the glassy alloys increases and the first peak positions of presently computed PDC show higher values, which shows strong dependence of the first-peak position of PDC on valence Z .

The PDC shows the existence of collective excitations at larger momentum transfer due to longitudinal phonons only and the instability of the transverse phonons due to the anharmonicity of the atomic vibrations in the metallic systems. Actually, neutron inelastic scattering (NIS) experiments on $\text{Mg}_{70}\text{Zn}_{30}$ glass by Suck et al. [15] have exposed clearly the low-lying short-wavelength collective density excitation at wave-vector transfer where the structure factor shows its main peak, which are called phonon-roton states [15]. The difference in the magnitude of the minimum around $2k_F$ seems to be due to the fact that the concept of roton has not been taken into account theoretically.

The anomalous behaviour of the specific heat is shown in Figs. 10–12 for $\text{Mg}_{70}\text{Zn}_{30}$, $\text{Mg}_{84}\text{Ni}_{16}$ and $\text{Mg}_{85.5}\text{Cu}_{14.5}$ metallic glasses, respectively. It is observed from Fig. 10 for the $\text{Mg}_{70}\text{Zn}_{30}$ glass that in the low-temperature region, on increasing the temperature T , the specific heat C_V computed from S-local field correction function shows high bump in all three approaches. For the $\text{Mg}_{70}\text{Zn}_{30}$ glass, the comparison of presently computed results for HB approach gives a qualitative agreement with the experimental data [15] available in the literature. But for the TG and BS approaches, the present results are lower for higher temperature. It is apparent from Fig. 11 that C_V for $\text{Mg}_{84}\text{Ni}_{16}$ glass is more sensitive to screening functions. The initial rise of the C_V values is observed in the low-temperature re-

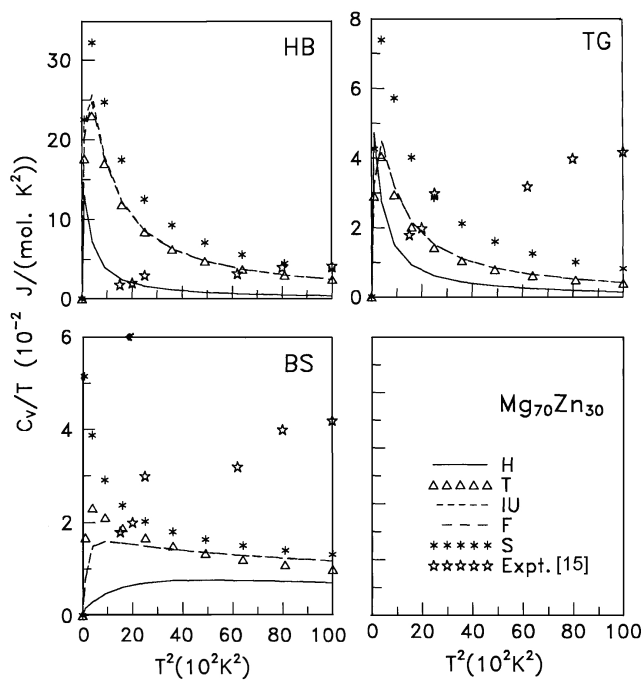


Fig. 10. Low-temperature specific heat of $Mg_{70}Zn_{30}$ glass using HB, TG and BS approaches. Legend: H – Hartree, T – Taylor, IU – Ichimaru-Utsumi, F – Farid et al., S – Sarkar et al.

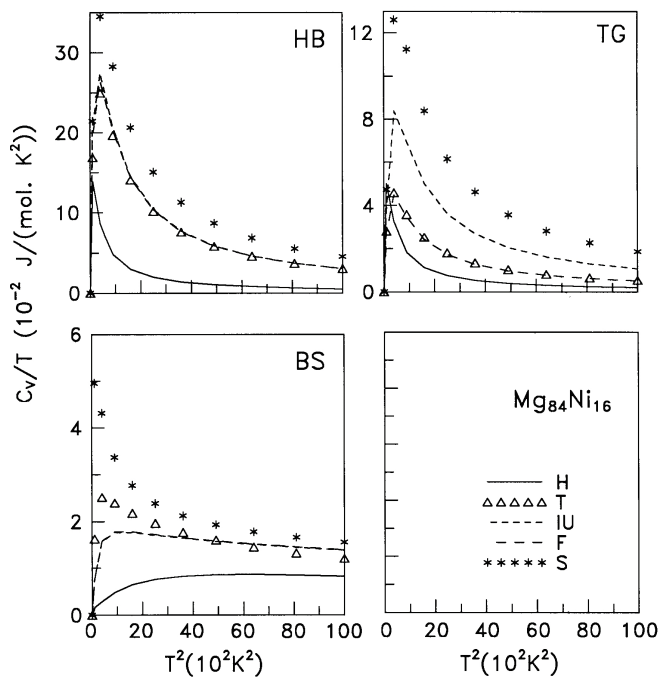


Fig. 11. Low-temperature specific heat of $Mg_{84}Ni_{16}$ glass using HB, TG and BS approaches. Legend: H – Hartree, T – Taylor, IU – Ichimaru-Utsumi, F – Farid et al., S – Sarkar et al.

gion, and for a further increase of the temperature, C_V converges. It is noted from Fig. 12 for the $Mg_{85.5}Cu_{14.5}$ glass that, as the temperature increases, C_V for the S-screening function shows a high bump in the low-temperature region. The HB approach produces stronger anomalous behaviour in the C_V curve compared to TG and BS approaches.

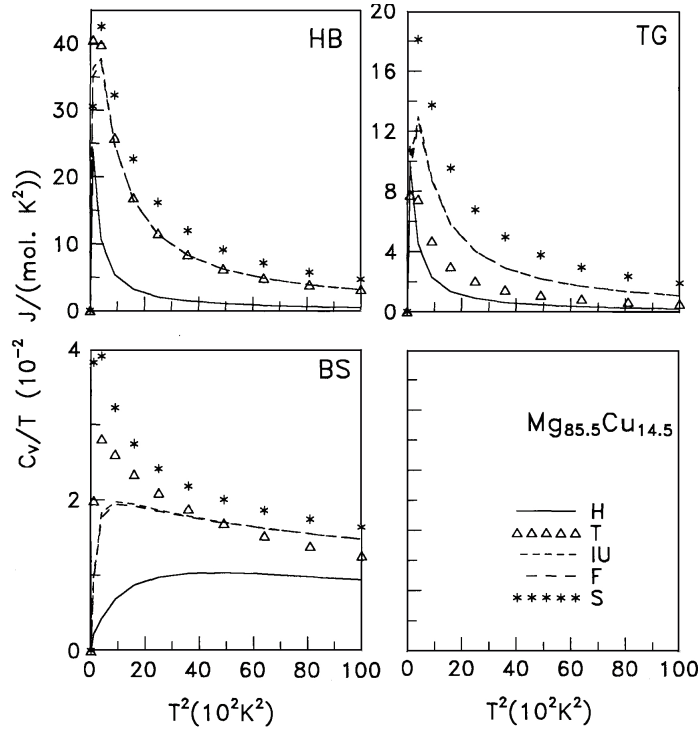


Fig. 12. Low-temperature specific heat of $Mg_{85.5}Cu_{14.5}$ glass using HB, TG and BS approaches. Legend: H—Hartree, T—Taylor, IU—Ichimaru-Utsumi, F—Farid et al., S—Sarkar et al.

As shown in Figs. 10–12, the exchange and correlation functions also affect the anomalous behaviour (i.e. deviation from the T^3 law) which is observed in the vibrational part of the specific heat C_V . The reason behind the anomalous behaviour may be due to the low frequency modes which modify the generalized vibrational density of states of the glass with that of the polycrystal. These modes are mainly responsible for the difference in the temperature dependence of the vibrational part of the specific heat which departs from the normal behaviour. The existence of a portion of the spectrum with ‘softer phonons’ (resembling rotons in liquid helium) may be the cause of anomalous behaviour of vibrational heat capacity C_V . In the low temperature region, a contribution to C_V is made by phonons of the initial part of the frequency spectrum. When the temperature reaches a value at which the energy of thermal motion becomes comparable to the minimum of energy of ‘softer phonons’, an additional contribution to heat capacity appears from the roton portion of $\omega(q)$.

A quantitative difference between the present calculation and the experimental results, in spite of good qualitative agreement, can be attributed to the following reasons: (1) the sampling conditions of the experiments, (2) the scarcity of data in the long wavelength region and (3) the low or high effectiveness of the local field correction functions used for the calculation of the pair potential.

From the overall picture of the present study, it can be noticed that the proposed model potential can be successfully applied to study the phonon dynamics of Mg-based metallic glasses. The influence of various local field correction functions is also observed. The experimental or theoretical data of $\text{Mg}_{84}\text{Ni}_{16}$ and $\text{Mg}_{85.5}\text{Cu}_{14.5}$ metallic glasses are not available in the literature, and the present study is very useful to form a set of theoretical data of the particular metallic glasses.

In all three approaches, it is very difficult to judge which approximation is the best for computation of phonon dynamics of Mg-based metallic glasses. The HB approach is the simplest and old one, it generates consistent results of the phonon data of these glasses, because the HB approximation needs minimum number of parameters. It has been found successful for generating the PDC of metallic glasses up to order of short wavelength density fluctuations. Also, this theory is based on random phase approximations, which gives a very satisfactory account of collective and individual particle motion and the interplay between them. However this approach is only applicable to systems in which the particle positions are not too highly correlated, a condition which is very poorly satisfied in the solids and not much better in the liquids. The TG approach is developed on the quasi-crystalline approximation in which effective force constant depends on the correlation function for the displacement of atoms, and the correlation function of displacement itself depends on the phonon frequencies. It is useful to compute the PDC of metallic glasses in high frequency collective modes. Basically, this theory deals with the study of phonon-like elementary excitations and the dispersion of this excitations depends on local order of the atoms by self constituent phonon scheme. The BS approach assumes a central force effective between the nearest neighbours and a volume dependence force due to the conduction electrons, hence, the disorderness of the atoms in the formation of metallic glasses is stronger, which results in a deviation in the magnitude of the PDC and the related properties. This model is applicable to most of the materials.

The thermodynamic and elastic properties have been computed from the elastic limit of the PDC and are reported in Tables 2–4. From Table 2, it is noted that the thermodynamic and elastic properties of $\text{Mg}_{70}\text{Zn}_{30}$ glass are not much affected by considering screening effects as in the cases of $\text{Mg}_{84}\text{Ni}_{16}$ and $\text{Mg}_{85.5}\text{Cu}_{14.5}$ metallic glasses. The longitudinal and transverse sound velocities of $\text{Mg}_{70}\text{Zn}_{30}$ glass in the BS approach show good agreement with the reported results [11]. For the $\text{Mg}_{84}\text{Ni}_{16}$ glass, calculated values of v_L , v_T , B_T , G , σ , Y and θ_D are displayed in Table 3. The results for $\text{Mg}_{84}\text{Ni}_{16}$ glass are not available in the literature, hence it is difficult to draw any remarks at this stage. The present results, computed from BS approach, show higher values than those of other two theoretical approaches. The calculated thermodynamic and elastic properties of $\text{Mg}_{85.5}\text{Cu}_{14.5}$ glass are shown in Table 4. It is noted from the table that the inclusion of exchange and correlation effects in the

TABLE 2. Thermodynamic and elastic properties of Mg₇₀Zn₃₀ metallic glass.

App.	SCR	v_L (km/s)	v_T (km/s)	B_T (GN/m ²)	G (GN/m ²)	σ	Y (GN/m ²)	θ_D (K)
HB	H	1.576	0.910	0.410	0.246	0.250	0.615	110.0
	T	1.645	0.950	0.446	0.268	0.250	0.670	114.8
	IU	1.535	0.886	0.389	0.233	0.250	0.583	107.1
	F	1.569	0.906	0.406	0.244	0.250	0.609	109.5
	S	1.530	0.883	0.386	0.232	0.250	0.579	106.8
TG	H	2.376	1.388	0.914	0.572	0.241	1.420	167.6
	T	3.278	1.915	1.738	1.090	0.242	2.704	231.3
	IU	3.138	1.869	1.542	1.037	0.225	2.542	225.3
	F	3.223	1.917	1.629	1.092	0.226	2.677	231.2
	S	3.067	1.796	1.516	0.958	0.239	2.375	216.9
BS	H	6.897	3.133	10.240	2.915	0.370	7.986	384.6
	T	5.559	1.350	8.455	0.541	0.469	1.590	167.9
	IU	5.782	1.704	8.779	0.862	0.453	2.504	211.4
	F	5.734	1.716	8.599	0.875	0.451	2.538	213.0
	S	5.376	0.886	8.273	0.234	0.486	0.694	110.4
Others [11]		4.7 5.1	2.5 2.6					305.21

static Hartree dielectric function enhanced the longitudinal and transverse sound velocities in the HB and TG approaches, while for the BS approach suppression of both velocities is observed. Theoretical and experimental data are not available in the literature for any comparison for the Mg_{85.5}Cu_{14.5} glass.

The dielectric function plays an important role in the evaluation of potential due to the screening of the electron gas. For this purpose, in the present investigations the local field correction functions due to H, T, IU, F and S are used. The reason for selecting these functions is that the H-function does not include exchange and correlation effect and represents only static dielectric function, while T-function covers the overall features of the various local field correction functions proposed before 1972. IU, F and S functions are recent ones among the existing functions and have not been exploited rigorously in such studies. This helps us to study the relative effects of exchange and correlation in the aforesaid properties. Hence, the five different local-field correction functions show variations up to an order of magnitude in the phonon properties.

TABLE 3. Thermodynamic and elastic properties of $Mg_{84}Ni_{16}$ metallic glass.

App.	SCR	v_L (km/s)	v_T (km/s)	B_T (GN/m ²)	G (GN/m ²)	σ	Y (GN/m ²)	θ_D (K)
HB	H	1.712	0.989	0.388	0.233	0.250	0.582	118.9
	T	1.796	1.037	0.427	0.256	0.250	0.641	120.8
	IU	1.686	0.973	0.376	0.226	0.250	0.565	117.1
	F	1.721	0.993	0.392	0.235	0.250	0.588	119.5
	S	1.661	0.959	0.365	0.219	0.250	0.548	115.4
TG	H	2.581	1.507	0.866	0.541	0.241	1.344	181.2
	T	3.546	2.071	1.634	1.022	0.241	2.537	248.9
	IU	3.416	2.034	1.465	0.987	0.225	2.417	244.1
	F	3.506	2.087	1.546	1.038	0.226	2.545	250.4
	S	3.323	1.948	1.427	0.904	0.238	2.239	234.0
BS	H	7.545	3.383	9.933	2.728	0.374	7.498	413.6
	T	6.115	1.470	8.227	0.515	0.469	1.513	181.9
	IU	6.343	1.853	8.499	0.819	0.453	2.380	229.0
	F	6.282	1.857	8.311	0.822	0.452	2.387	229.4
	S	5.913	0.994	8.106	0.236	0.486	0.700	123.3

TABLE 4. Thermodynamic and elastic properties of $Mg_{85.5}Cu_{14.5}$ metallic glass.

App.	SCR	v_L (km/s)	v_T (km/s)	B_T (GN/m ²)	G (GN/m ²)	σ	Y (GN/m ²)	θ_D (K)
HB	H	1.264	0.730	0.206	0.123	0.250	0.308	86.8
	T	1.371	0.791	0.242	0.145	0.250	0.363	94.2
	IU	1.416	0.818	0.258	0.155	0.250	0.387	97.3
	F	1.432	0.827	0.264	0.159	0.250	0.396	98.4
	S	1.503	0.868	0.291	0.175	0.250	0.436	103.2
TG	H	1.859	1.083	0.438	0.272	0.243	0.676	128.8
	T	2.609	1.519	0.865	0.535	0.244	1.330	180.5
	IU	2.582	1.542	0.810	0.551	0.223	1.348	182.9
	F	2.644	1.578	0.851	0.577	0.223	1.413	187.2
	S	2.571	1.518	0.820	0.534	0.233	1.316	180.2
BS	H	6.959	3.107	8.243	2.237	0.376	6.155	375.6
	T	5.828	1.421	7.250	0.468	0.468	1.375	173.9
	IU	6.077	1.787	7.575	0.741	0.453	2.152	218.3
	F	6.048	1.821	7.454	0.769	0.450	2.229	222.3
	S	5.633	1.138	6.955	0.300	0.479	0.888	139.4

4. Conclusion

The PDC generated from three approaches with five local-field correction functions reproduce all main characteristics of the dispersion curves. The well recognized model potential with more advanced F and S local-field correction functions generates consistent results. The experimental and theoretical data for $\text{Mg}_{84}\text{Ni}_{16}$ and $\text{Mg}_{85.5}\text{Cu}_{14.5}$ glasses are not available in the literature. Therefore, it is difficult to draw any special conclusions. However, the present study is very useful to provide important information regarding the particular glasses. Also, the present computation confirms the applicability of the model potential in the aforesaid properties and supports the present approach of PAA. The study on phonon dynamics of other binary liquid alloys and metallic glasses is in progress.

References

- [1] P. N. Gajjar, A. M. Vora and A. R. Jani, Proc. 9th Asia Pacific Physics Conf., Hanoi, Vietnam (October 25-31, 2004), The Gioi Publication (2006) 429.
- [2] A. M. Vora, Chinese Phys. Lett. **23** (2006) 1872; J. Non-Cryst. Sol. **352** (2006) 3217; J. Mater. Sci. **43** (2007) 935; Acta Phys. Pol. A **111** (2007) 859; Front. Mater. Sci. China **1** (2007) 366.
- [3] A. M. Vora, M. H. Patel, P. N. Gajjar and A. R. Jani, Solid State Phys. **46** (2003) 315.
- [4] B. Y. Thakore, P. N. Gajjar and A. R. Jani, Solid State Phys. (India) C **40** (1997) 70; Bull. Mater. Sci. **23** (2000) 5.
- [5] J. Hubbard and J. L. Beeby, J. Phys. C: Solid State Phys. **2** (1969) 556.
- [6] S. Takeno and M. Goda, Prog. Theor. Phys. **45** (1971) 331; Prog. Theor. Phys. **47** (1972) 790.
- [7] A. B. Bhattia and R. N. Singh, Phys. Rev. B **31** (1985) 4751.
- [8] M. M. Shukla and J. R. Campanha, Acta Phys. Pol. A **94** (1998) 655.
- [9] L. von Heimendahl, J. Phys F: Met. Phys. **9** (1979) 161.
- [10] D. Tomanek, Diplomarbeit, Universität Basel (1979).
- [11] N. S. Saxena, D. Bhandari, A. Pratap and M. P. Saksena, J. Phys: Condens Matter **2** (1990) 9475.
- [12] N. S. Saxena, K. C. Jain, N. Gupta and M. P. Saksena, Physica B **174** (1991) 136.
- [13] P. C. Agarval, K. A. Aziz and C. M. Kachhava, Acta Phys. Hung. **72** (1992) 183; Phys. Stat Sol (b) **178** (1993) 303.
- [14] P. C. Agarval and C. M. Kachhava, Physica B **179** (1992) 43; Phys. Stat. Sol. (b) **179** (1993) 365.
- [15] J.-B. Suck, H. Rudin, H.-J. Günterodt and H. Beck, J. Phys. C: Solid State Phys. **13** (1980) L1045.
- [16] J. Hafner and S. S. Jaswal, Phil. Mag. A **58** (1988) 61.
- [17] J. Hafner, S. S. Jaswal, M. Tegze, A. Pflugi, J. Krieg, P. Oelhafen and H.-J. Günterodt, J. Phys. F: Met. Phys. **18** (1988) 2583.
- [18] C. J. Benmore, B. J. Oliver, J.-B. Suck, R. A. Robinson and P. A. Eglestaff, J. Phys.: Condens. Matter **7** (1995) 4775.

- [19] C. J. Benmore, S. Sweeney, R. A. Robinson, P. A. Eglestaff and J.-B. Suck, *Physica B* **241-243** (1998) 912; *J. Phys.: Condens. Matter* **11** (1999) 7079.
- [20] T. Bryk and I. Mryglod, *Cond. Mat. Phys.* **2** (1999) 285.
- [21] E. Nassif, P. Lamparter and S. Steeb, *Z. Naturforsch.* **38a** (1983) 1206.
- [22] E. Nassif, P. Lamparter W. Sperl and S. Steeb, *Z. Naturforsch.* **38a** (1983) 142.
- [23] W. A. Harrison, *Pseudopotentials in the Theory of Metals*, W. A. Benjamin, New York (1966).
- [24] R. Taylor, *J. Phys. F: Met. Phys.* **8** (1978) 1699.
- [25] S. Ichimaru and K. Utsumi, *Phys. Rev. B* **24** (1981) 3220.
- [26] B. Farid, V. Heine, G. E. Engel and I. J. Robertson, *Phys. Rev. B* **48** (1993) 11602.
- [27] A. Sarkar, D. S. Sen, S. Haldar and D. Roy, *Mod. Phys. Lett. B* **12** (1998) 639.
- [28] N. P. Kovalenko and Yu. P. Krasny, *Physics B* **162** (1990) 115.

RAČUNANJE FONONSKE DISPERZIJE U NEKRISTALNIM
MAGNEZIJEVIM LEGURAMA

Primjenom poznatog potencijala Gajjar-a i sur., izračunali smo fononske disperzijske funkcije (FDF) i fizička svojstva triju metalnih stakala na bazi magnezija, $Mg_{70}Zn_{30}$, $Mg_{84}Ni_{16}$ i $Mg_{85.5}Cu_{14.5}$. Prvi puta primjenjuje se model pseudo-leguratom umjesto Vegardovog modela. Primijenili smo tri teorijska pristupa, Hubbard-Beeby-ev, Takeno-Goda-ov i Bhatia-Singh-ov za izračunavanje FDF. Radi nalaženja učinaka izmjene i korelacija, prvi smo uveli pet funkcija za popravke lokalnog polja, prema autorima Hartree-u, Taylor-u, Ichimaru-Utsumi-u, Farid-a i sur. te Sarkar-a i sur. radi nalaženja učinaka izmjene i korelacija. Izračunali smo termodinamička i elastična svojstva na osnovi elastične granice FDF i nalazimo dobar sklad s objavljenim teorijskim i eksperimentalnim podacima. Ishodi za FDF legure $Mg_{70}Zn_{30}$ su u razumnom skladu s teorijskim i eksperimentalnim podacima.